Injectable enzymatically crosslinked hydrogels based on a poly(L-glutamic acid) graft copolymer

ARTICLE *in* POLYMER CHEMISTRY · JUNE 2014

Impact Factor: 5.52 · DOI: 10.1039/C4PY00420E

5 AUTHORS, INCLUDING:

Kaixuan Ren
Harvard University
4 PUBLICATIONS **37** CITATIONS
SEE PROFILE

Yilong Cheng
University of Washington Seattle
18 PUBLICATIONS **364** CITATIONS
SEE PROFILE

Polymer Chemistry

PAPER

Injectable enzymatically crosslinked hydrogels based on a poly(L-glutamic acid) graft copolymer†

Kaixuan Ren,[ab] Chaoliang He,*[a] Yilong Cheng,[a] Gao Li*[a] and Xuesi Chen[a]

Cite this: *Polym. Chem.*, 2014, **5**, 5069

Received 24th March 2014
Accepted 5th May 2014

DOI: 10.1039/c4py00420e

www.rsc.org/polymers

Enzymatically crosslinked injectable hydrogels based on poly(L-glutamic acid) grafted with tyramine and poly(ethylene glycol) (denoted as PLG-*g*-TA/PEG) were developed under physiological conditions in the presence of horseradish peroxidase (HRP) and hydrogen peroxide (H_2O_2). Their gelation time, mechanical properties, swelling behaviors and porous structure were evaluated. The hydrogels were rapidly formed in the presence of low concentrations of HRP and H_2O_2. The storage modulus of the hydrogels could be well controlled and increased by increasing the concentrations of HRP and H_2O_2. The average pore-size of the hydrogels varied from 20 to 120 μm, depending on the H_2O_2 concentration. In addition, the encapsulated L929 fibroblast cells in the PLG-*g*-TA/PEG hydrogels exhibited high viability. After subcutaneous injection of the PLG-*g*-TA/PEG solutions containing HRP and H_2O_2 into the back of rats, the hydrogels were rapidly formed *in situ*. The hydrogels were found to persist for up to 10 weeks *in vivo*, and histological analysis indicated that the hydrogels exhibited acceptable biocompatibility. These results suggested that the biocompatible, injectable enzyme-mediated PLG-*g*-TA/PEG hydrogels are promising for biomedical applications including tissue engineering scaffolds and drug delivery carriers.

Introduction

Hydrogels are three-dimensional (3D) hydrophilic polymer networks retaining a large amount of water. Due to their high water content and physical properties that resemble the native extracellular matrix (ECM), hydrogels have drawn considerable attention for biomedical applications, such as tissue engineering scaffolds and drug delivery carriers.[1–5] Injectable hydrogels exhibit unique advantages, such as excellent permeability for nutrients and metabolites, good biocompatibility and minimally invasive injection procedures. The encapsulation of cells, drugs, and bioactive molecules into the hydrogels can be easily achieved. Until now, various crosslinking approaches, including physical and chemical crosslinking, have been developed to construct hydrogels *in situ*. Physically crosslinked hydrogels are formed based on non-covalent interactions, such as ionic interactions,[6,7] hydrogen bonds,[8] hydrophobic interactions,[9] and stereo-complexations.[10,11] They are usually reversible networks with relatively low mechanical properties. On the other hand, chemically crosslinked hydrogels are covalent networks formed *via* chemical reactions, including radical polymerization,[12,13] Michael-type addition reaction,[14–16] or Schiff-base reaction.[17]

Recently, increasing attention has been paid to enzymatically crosslinked hydrogels for biomedical applications due to their good biocompatibility, fast gelation process and tunable mechanical properties. Horseradish peroxidase (HRP) is the most widely used enzyme for enzymatically crosslinked hydrogels because of its high stability and good biocompatibility.[18] HRP is a hemoprotein that catalyzes the coupling of aniline or phenol derivatives *via* a carbon–carbon bond or a carbon–nitrogen/oxygen bond in the presence of hydrogen peroxide.[18] Additionally, the physiochemical properties of hydrogels, such as gelation rate, mechanical strength and porous structure, are easy to control by modulation of the HRP activity. Considerable studies on HRP-mediated *in situ* forming hydrogels have been focused on naturally derived materials, such as hyaluronic acid,[19–21] alginate,[22,23] dextran,[24–27] gelatin[28–31] and chitosan.[32–36] These hydrogels have shown potential in biomedical applications due to their cell-interactive properties and biodegradability. Very recently, the enzymatically crosslinked hydrogels based on synthetic polymers have attracted increasing interest due to their advantages including tunable mechanical properties and low immunogenicity. For instance, the injectable hydrogels based on tyramine-conjugated 4-arm poly(propylene oxide)–poly(ethylene oxide) (PPO–PEO) *via* enzyme-catalyzed crosslinking have been developed.[37–40] These hydrogels displayed good cytocompatibility and degraded rapidly in 6 days *in vitro*.[38]

[a]*Key Laboratory of Polymer Ecomaterials, Changchun Institute of Applied Chemistry, Chinese Academy of Sciences, Changchun 130022, P. R. China. E-mail: clhe@ciac.ac.cn; ligao@ciac.ac.cn*

[b]*University of Chinese Academy of Sciences, Beijing 100039, P. R. China*

† Electronic supplementary information (ESI) available. See DOI: 10.1039/c4py00420e

Among various synthetic polymers, synthetic polypeptides have attracted extensive interest due to their excellent biocompatibility, biodegradability, and structures mimicking natural proteins.[41,42] In addition, the reactive side groups in some polypeptides facilitate further functionalization. These properties lead to unique advantages of polypeptides in biomedical applications. Nevertheless, to date, reports on injectable enzymatically crosslinked hydrogels based on polypeptides have still been limited. In the present work, a type of injectable hydrogel based on poly(L-glutamic acid) grafted with tyramine and poly(ethylene glycol) (denoted as PLG-*g*-TA/PEG) was prepared under physiological conditions in the presence of horseradish peroxidase (HRP) and hydrogen peroxide (H_2O_2). The PLG-*g*-TA/PEG copolymers were synthesized *via* an amidation reaction. The chemical structures of the copolymers were characterized by ^{1}H NMR and UV-Vis spectroscopy. The physicochemical properties of the hydrogels, such as gelation time, mechanical properties, swelling behaviors and porous structure, were studied in detail. The viability and proliferation of L929 fibroblast cells in the hydrogels were evaluated by the live–dead assay and the cell counting kit-8 (CCK-8) method. Moreover, the biodegradability and biocompatibility of the hydrogels *in vivo* were further investigated by subcutaneous injection of the hydrogels into the back of rats.

Experimental

Materials

Poly(ethylene glycol) monomethyl ether (mPEG, $M_n = 2000$) was purchased from Aldrich. The amino-terminated poly(ethylene glycol) monomethyl ether (mPEG-NH_2) was synthesized according to the literature procedure.[43,44] γ-Benzyl-L-glutamate-*N*-carboxyanhydride (BLG NCA) was synthesized according to the previously reported method.[45] *N*-Ethyl-*N*′-(3-dimethylaminopropyl) carbodiimide hydrochloride (EDC) (GL Biochem), *N*-hydroxysuccinimide (NHS) (GL Biochem), tyramine hydrochloride (TA) (Aladdin), HBr solution (33 wt%) in acetic acid (J&K Scientific Ltd) and dichloroacetic acid ($CHCl_2COOH$) (J&K Scientific Ltd) were used as received. Horseradish peroxidase (HRP, 200 units per mg) was purchased from Aldrich and used without further purification. Tetrahydrofuran (THF) and dioxane were refluxed with sodium and distilled under nitrogen prior to use. All the other reagents and solvents were of analytical grade and used as obtained.

Characterization

^{1}H NMR spectra were recorded on a Bruker AV 400 NMR spectrometer. The molecular weights and polydispersity indices (PDI) of poly(L-glutamic acid) were determined by gel permeation chromatography (GPC) using a Waters linear Ultrahydrogel column and a Waters 1515 isocratic HPLC pump with a Waters 2414 refractive index detector. The eluent was 0.2 M phosphate buffer (PB) containing 0.1 M NaN_3 at a flow rate of 1.0 mL min^{-1} at 25 °C. Monodispersed PEG standards purchased from Waters Co. with a molecular weight ranging from 3000 to 1.0×10^5 were used to generate the calibration curve. The content of conjugated phenol groups within the copolymer was measured by using an ultraviolet-visible (UV-Vis) spectrometer (UV-2401PC, Shimadzu, Kyoto, Japan). The PLG-*g*-TA/PEG copolymer was dissolved in 1 mg mL^{-1} of distilled water and the absorbance at 277 nm was measured. The content of conjugated phenol groups was calculated from a calibration curve obtained by measuring the absorbance of tyramine hydrochloride at different concentrations in distilled water. The ellipticity of polymer aqueous solution (0.5 g L^{-1}, pH = 7.4) was obtained on a JASCO J-810 spectrometer at 25 °C.

Synthesis of poly(L-glutamic acid) (PLG)

Poly(γ-benzyl-L-glutamate) (PBLG) was synthesized according to our previously reported method.[45] Typically, BLG NCA (10.3 g, 39 mmol) was dissolved in anhydrous dioxane under a nitrogen atmosphere, and triethylamine (TEA, 17.6 μL, 0.13 mmol) was then added. The reaction mixture was allowed to stir at 25 °C for three days. Then the polymer was purified by precipitation into cold diethyl ether, followed by filtration. The obtained product was further purified with diethyl ether and dried under vacuum. PBLG was obtained with a yield of 72%. Poly(L-glutamic acid) (PLG) was obtained by deprotection of PBLG. Briefly, PBLG (5 g) was dissolved in 50 mL of $CHCl_2COOH$, followed by addition of 15 mL of HBr solution (33 wt%) in acetic acid. The reaction mixture was stirred at 30 °C for two hours. The product was obtained by precipitation in diethyl ether, washed repeatedly with diethyl ether and dried under vacuum. After dissolving the product in DMSO, the solution was dialyzed against deionized water for 3 days (MWCO 7000 Da). PLG was collected by lyophilization with a yield of 87%.

Synthesis of poly(L-glutamic acid)-*graft*-tyramine/poly(ethylene glycol) (PLG-*g*-TA/PEG)

The PLG-*g*-TA/PEG copolymer was prepared by coupling PLG with TA and mPEG-NH_2 *via* EDC–NHS activated amidation reaction. PLG (1.5 g, 11.6 mmol of COOH groups) was first dissolved in 40 mL of DMSO. The carboxyl groups of PLG were activated using EDC–NHS (COOH : EDC : NHS = 1 : 0.6 : 0.6 (molar ratio)). TA (0.5 g, 2.9 mmol) and mPEG-NH_2 (7.0 g, 3.5 mmol) were then added and the resulting solution was stirred for two days at room temperature. The product was purified by dialysis against deionized water for 3 days (MWCO 7000 Da). The final product, PLG-*g*-TA/PEG copolymer, was collected as a white solid by lyophilization with a yield of 83%.

Gelation time

Enzymatically crosslinked PLG-*g*-TA/PEG hydrogels (300 μL) were prepared in the presence of HRP and H_2O_2 at room temperature. The final concentration of PLG-*g*-TA/PEG was fixed at 6.7% (w/v) (Fig. S1 in the ESI†). To evaluate the dependence of gelation time on the HRP and H_2O_2 concentrations, the polymer solution (200 μL, 10% (w/v)) in 0.01 M PBS (pH 7.4) was mixed with different concentrations of HRP solution (50 μL) and H_2O_2 solution (50 μL) in 5 mL vials, and then the mixture was gently shaken. The gelation time of the PLG-*g*-TA/PEG hydrogels was determined using the vial tilting method. The sample was

considered to be in a gel state if no flow was observed within 30 s after inverting the vial.

Rheological experiments

Rheological experiments of the hydrogels were performed on a US 302 Rheometer (Anton Paar) using a parallel plate (plate diameter = 25 mm, gap = 0.5 mm) in oscillatory mode at 37 °C. For the measurements, 200 μL of the PLG-*g*-TA/PEG solution (10% (w/v)) was mixed with different concentrations of HRP solution (50 μL) and H_2O_2 solution (50 μL), and then placed on the plate of the rheometer immediately. The storage modulus (G') and loss modulus (G'') were recorded as a function of time at a frequency of 1 Hz and a strain of 1%. The sample was sealed by a thin layer of silicon oil to prevent the evaporation of water.

Morphology of the hydrogels

To elucidate the morphology of hydrogels, the samples were frozen rapidly by plunging them into liquid nitrogen and then freeze-dried for two days. The specimens were cross-sectioned and sputter coated with gold. The morphology of the specimens was observed by scanning electron microscopy (Micrion FEI PHILIPS).

Swelling ratio

Hydrogels were prepared in vials according to the procedure above. The freeze-dried hydrogels were accurately weighed (W_0) and then incubated in 10 mL of PBS solution at 37 °C. At predetermined time intervals, the buffer solutions were removed completely and the remaining samples were weighed (W_t) to calculate the swelling ratio (SR), which is defined as $(W_t - W_0)/W_0$. The experiments were performed in triplicate.

In vitro cytocompatibility

The cell viability and proliferation of the hydrogels were evaluated by 3D culture of L929 mouse fibroblasts inside the hydrogels. Cells were cultured in Dulbecco's modified Eagle's medium (DMEM) containing 10% fetal bovine serum, supplemented with 50 U mL^{-1} penicillin and 50 U mL^{-1} streptomycin and incubated at 37 °C and in a 5% CO_2 atmosphere. All the sample solutions were sterilized by filtrating *via* 0.2 μm syringe filters. First, PLG-*g*-TA/PEG solution (10% (w/v), 200 μL) was mixed with harvested cells (1×10^5 cells) and put into the well of a 24-well plate, and then 50 μL of HRP solution and 50 μL of H_2O_2 solution were added into the well. 1 mL of DMEM was added after the hydrogel was formed. The viability of encapsulated L929 cells at 24 h was determined by using a live–dead cell staining kit. In brief, 500 μL of PBS solution containing 2 μM calcein AM and 4 μM propidium iodide (PI) was added and the sample was further incubated at 37 °C for 30 min. The sample was observed using a fluorescent microscope after removing the staining solution. Viable cells were stained green with calcein AM, and dead cells were stained red with PI. In addition, the proliferation of L929 cells in the hydrogels was assessed by the cell counting kit-8 (CCK-8) method ($n = 3$). At predetermined period, CCK-8 solution (1.0 mL, 10% v/v in medium) was added into each well of the plate. After 4 h incubation, the absorbance value at 450 nm was measured with an ELISA reader (Tecan Infinite M200). The absorbance at 600 nm was used for baseline correction. The cytotoxicity of the hydrogels and any leachable materials was also evaluated by using methyl thiazolyl tetrazolium (MTT) assay. Briefly, L929 cells were seeded at a density of 10^4 per well in a 96-well plate and incubated for 24 h. The medium was replaced by the eluent of hydrogels or PEI 25K solution with a concentration of 0.125 mg mL^{-1}, which was used as a positive control. The cells were subjected to MTT assay after being incubated for another 24 h. The absorbance value at 490 nm was measured using a microplate reader. Cell viability (%) was calculated according to the following equation: viability (%) = $(A_{sample})/(A_{control}) \times 100\%$, where A_{sample} and $A_{control}$ are the absorbance of the sample and the control well (without the eluent of hydrogels), respectively. The measurements were performed in triplicate.

In vivo degradation and biocompatibility

Sprague-Dawley (SD) rats (~200 g) were used for *in vivo* tests. Rats were anesthetized by inhalation of diethyl ether. PLG-*g*-TA/PEG solutions (10% (w/v), 500 μL for each sample) in PBS containing H_2O_2 (1.6 mM) and HRP (2 units per mL) were subcutaneously injected into the back of the rats. At predetermined time intervals, the rats were euthanized, and the gel status was observed. The tissues surrounding the injection sites were surgically removed and stored in neutral buffered formalin solution (NBF). The histology analysis was examined by staining with hematoxylin and eosin (H&E).

Animal procedure

The animal experiments were carried out according to the guide for the care and use of laboratory animals, provided by Jilin University, Changchun, China, and the procedure was approved by the local Animal Ethics Committee.

Results and discussion

Synthesis and characterization of the PLG-*g*-TA/PEG copolymer

The synthetic route to the PLG-*g*-TA/PEG copolymer is illustrated in Scheme 1. Poly(L-glutamic acid) (PLG) was synthesized by ring-opening polymerization (ROP) of BLG NCA with triethylamine as an initiator, followed by deprotection of the benzyl groups of PBLG using HBr solution (33 wt%) in acetic acid. Subsequently, TA and mPEG-NH_2 were grafted to the backbone of PLG *via* a carbodiimide active amidation reaction. The typical ^1H NMR spectra are shown in Fig. 1. The disappearance of the peak of benzyl groups in PLG suggested the successful deprotection of PBLG (Fig. 1A and B). The weight-average molecular weight (M_w) of PLG was evaluated to be 1.3×10^4 with a polydispersity index (PDI) of 1.28 by GPC. Based on the ^1H NMR spectrum of the graft copolymer (Fig. 1C), in addition to the typical peaks assigned to PLG, the representative peaks ascribed to tyramine (TA) and PEG were also observed, indicating the successful synthesis of the PLG-*g*-TA/PEG copolymer. The

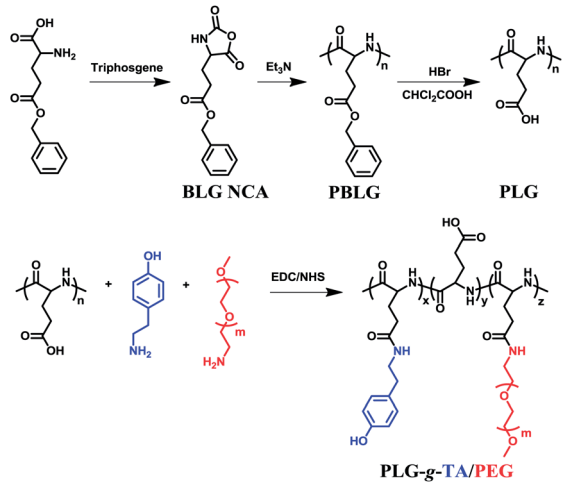

Scheme 1 Synthetic route to the PLG-*g*-TA/PEG copolymer.

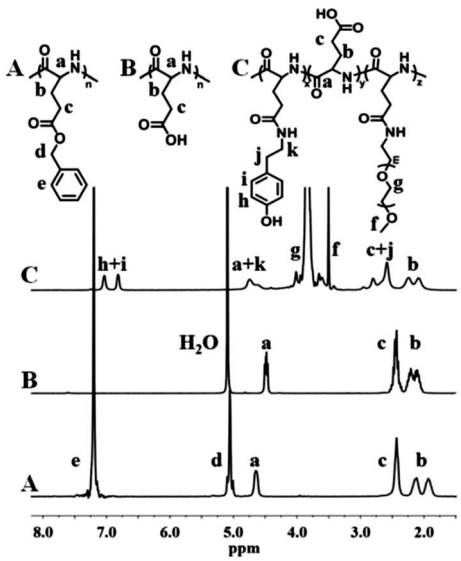

Fig. 1 ^{1}H NMR spectra of (A) PBLG in CF_3COOD; (B) PLG in D_2O; (C) PLG-*g*-TA/PEG copolymer in CF_3COOD.

grafting ratio of TA residues, defined as the number of TA moieties per 100 repeated units of L-glutamate, was calculated to be 20 by comparing the integration of the peak of TA (–C_6H_4–) at 6.8–7.0 ppm with that of the methylene peak of the glutamate unit (–CH_2CH_2C(O)–) at about 2.1 ppm (Fig. 1C). Similarly, the grafting ratio of mPEG-NH_2 residues was calculated to be 28 based on the NMR results. The weight contents of TA and PEG were 3.9 wt% and 79.1 wt%, respectively. The conjugation of TA with PLG was also examined by using a UV-Vis spectrometer. The PLG-*g*-TA/PEG aqueous solution showed a specific absorbance peak at 277 nm, which corresponds to the absorbance of phenol moieties (Fig. 2a). The content of conjugated TA was 4.5 wt%, which is consistent with the NMR results. Additionally, the conformation of PLG-*g*-TA/PEG in aqueous solution at pH 7.4 was examined by circular dichroism spectroscopy. As shown in Fig. 2b, a small positive maximum at about 217 nm and a large minimum at about 204 nm were observed, indicating that PLG-*g*-TA/PEG adopted a random conformation.[46] The reason could be attributed to the fact that the residue carboxyl groups of PLG were in ionized form at pH 7.4.[46]

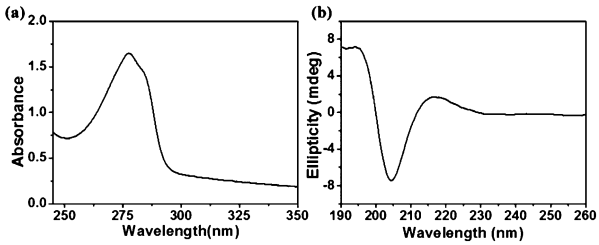

Fig. 2 (a) UV-Vis absorbance spectrum of PLG-*g*-TA/PEG aqueous solution; (b) circular dichroism spectrum of PLG-*g*-TA/PEG aqueous solution (pH 7.4).

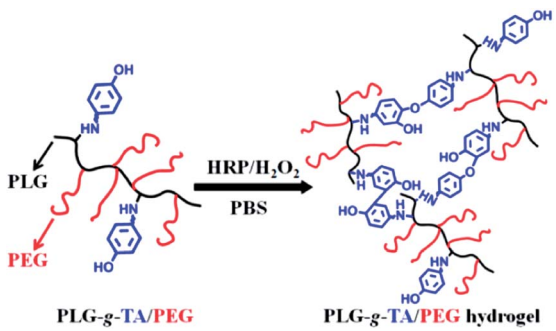

Scheme 2 Schematic route of enzyme-mediated crosslinking of the PLG-*g*-TA/PEG copolymer.

Preparation and gelation time of the hydrogels

The hydrogels were prepared by HRP-mediated crosslinking of the PLG-*g*-TA/PEG copolymer (Scheme 2). The coupling of phenol moieties in the PLG-*g*-TA/PEG copolymer *via* the carbon–carbon bonds or carbon–oxygen bonds was catalyzed by HRP and H_2O_2, leading to the formation of intermolecular covalent linkages and the rapid formation of hydrogels. The gelation time was determined by the vial tilting method. The dependence of the gelation time on the concentrations of HRP and

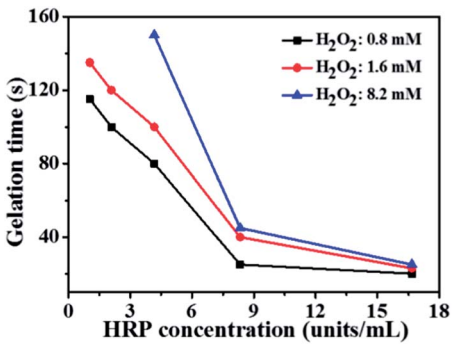

Fig. 3 Dependence of gelation time of PLG-*g*-TA/PEG hydrogels on HRP and H_2O_2 concentrations.

H_2O_2 is shown in Fig. 3. The gelation time reduced from 135 to 23 s as the HRP concentration increased from 1.0 to 16.7 units per mL at a fixed polymer concentration of 6.7% (w/v) and a H_2O_2 concentration of 1.6 mM. This should be attributed to the fact that the increase in HRP concentration accelerated the generation of phenolic free radicals.[25,38] In contrast, as the H_2O_2 concentration increased from 0.8 to 8.2 mM, the gelation time prolonged from 80 to 150 s at a fixed HRP concentration of 4 units per mL. This phenomenon occurred due to the inhibition effect of excessive H_2O_2 on the activity of HRP.[38] The influence of HRP and H_2O_2 concentrations on the gelation time was consistent with some naturally derived systems, such as carboxymethylcellulose[47,48] and gelatin.[28,29] Notably, the hydrogels based on PLG-*g*-TA/PEG have been developed by using relatively low amounts of H_2O_2, which may avoid toxic effects of H_2O_2 at high concentrations.[49] Additionally, it was found that the gelation time of PLG-*g*-TA/PEG hydrogels was tunable by changing the concentrations of HRP and H_2O_2. The control of the gelation time is quite important for practical applications of the hydrogels.

Rheological experiments

The viscoelastic property of PLG-*g*-TA/PEG hydrogels was measured in a time-controlled oscillatory mode at 37 °C. A mixture of PLG-*g*-TA/PEG, HRP and H_2O_2 solutions in PBS was placed on the plate of rheometer. The formation of hydrogels was detected by monitoring the variations of storage modulus (G') and loss modulus (G'') with time. As shown in Fig. 4a, the G' and G'' of PLG-*g*-TA/PEG hydrogels crosslinked with 2 units per mL of HRP and 1.6 mM of H_2O_2 were measured as a function of time. An immediate gelation was observed as soon as the mixture was placed on the plate of rheometer. Subsequently, the storage modulus of the hydrogels gradually increased during the initial stage and eventually reached a plateau, suggesting that the crosslinking reaction was complete.[20] As shown in Fig. 4b, the storage modulus of PLG-*g*-TA/PEG hydrogels strengthened from 1600 to 2300 Pa by increasing the concentration of HRP from 1 to 4 units per mL at a fixed H_2O_2 concentration of 1.6 mM. This result indicated that HRP displayed a marked effect on the mechanical properties of the hydrogels.[40] Notably, the increase in H_2O_2 concentration led to a higher storage modulus. This should be due to the fact that H_2O_2 acted as a crosslinker in this system and therefore the

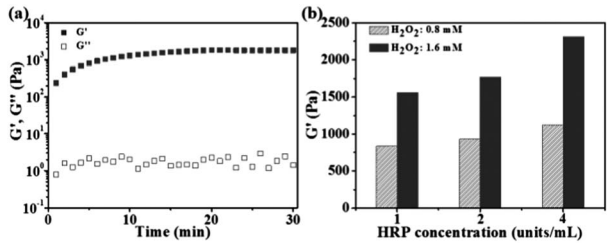

Fig. 4 (a) Storage modulus (G') and loss modulus (G'') of PLG-*g*-TA/PEG hydrogels as a function of time in the presence of 2 units per mL of HRP and 1.6 mM of H_2O_2; (b) the effects of HRP and H_2O_2 concentrations on G' of PLG-*g*-TA/PEG hydrogels.

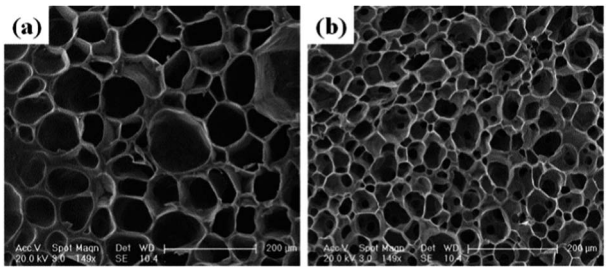

Fig. 5 SEM images of lyophilized PLG-*g*-TA/PEG hydrogels crosslinked with (a) 0.8 mM of H_2O_2 and 2 units per mL of HRP, or (b) 1.6 mM of H_2O_2 and 2 units per mL of HRP. The scale bar represents 200 μm.

increase in H_2O_2 concentration led to the increase in the crosslinking density.[38] The results of rheological tests demonstrated that the mechanical properties of the hydrogels could be controlled by varying the HRP and H_2O_2 concentrations.

Morphology of lyophilized hydrogels

The morphology of lyophilized hydrogels was observed by SEM. As shown in Fig. 5, the PLG-*g*-TA/PEG hydrogels exhibited interconnected porous structures. It was found that the pore size of the hydrogels was markedly influenced by the H_2O_2 concentration. For instance, the average pore-size of the hydrogel crosslinked with 0.8 mM of H_2O_2 and 2 units per mL of HRP ranged from 70 to 120 μm (Fig. 5a). In contrast, the inner porous structure of the hydrogel crosslinked with 1.6 mM of H_2O_2 and 2 units per mL of HRP was more compact and the average pore-size ranged from 20 to 60 μm (Fig. 5b). The decrease in the pore size as the increase in H_2O_2 concentration was due to a higher cross-linking density.[38] It is noteworthy that many studies have demonstrated that the porous micro-structure with a suitable pore size of the hydrogel matrix played a critical role in cell survival, migration, proliferation and differentiation.[50] Furthermore, the pore size of hydrogels affected the release behaviors of encapsulated drugs or bioactive molecules.[21] In our study, the pore size of the PLG-*g*-TA/PEG hydrogels could be easily adjusted by the H_2O_2 concentration, which contributed to the further applications of the PLG-*g*-TA/PEG hydrogels.

Swelling ratio of the hydrogels

The swelling behaviors of PLG-*g*-TA/PEG hydrogels formed with various HRP and H_2O_2 concentrations were determined by incubating the freeze-dried hydrogels in PBS at 37 °C. The hydrogels were weighed at predetermined time intervals to obtain the swelling ratios. As shown in Fig. 6, the hydrogels had a high equilibrium swelling ratio ranging from 33 to 49, suggesting that freeze-dried PLG-*g*-TA/PEG hydrogels absorbed plenty of water because of the hydrophilic PEG segments. It was found that the equilibrium swelling ratio reduced as the H_2O_2 concentration increased from 0.8 to 1.6 mM (Fig. 6a and S2 in the ESI†). Additionally, with the increase of HRP concentration from 2 to 8 units per mL, the equilibrium swelling ratio decreased from 49 to 40 (Fig. 6b). Generally, the swelling ratio is

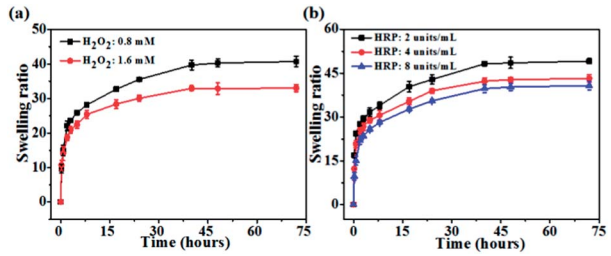

Fig. 6 Swelling ratios of PLG-*g*-TA/PEG hydrogels: (a) HRP concentration fixed at 8 units per mL; (b) H_2O_2 concentration fixed at 0.8 mM ($n = 3$).

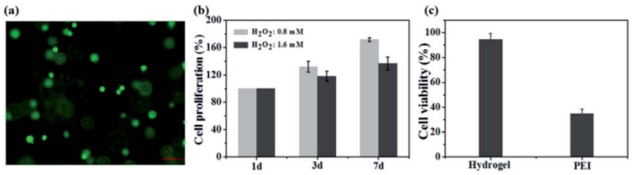

Fig. 7 *In vitro* 3D culture of L929 cells. (a) Viability of L929 cells in the PLG-*g*-TA/PEG hydrogel in the presence of 1.6 mM of H_2O_2 and 2 units per mL of HRP after 1 day incubation. Cells were stained with calcein-AM and PI. Live and dead cells show green and red fluorescence, respectively. The scale bar represents 100 μm. (b) Proliferation of L929 cells in the PLG-*g*-TA/PEG hydrogels analyzed by the CCK-8 method. (c) Cell viability after exposure to the eluent of the PLG-*g*-TA/PEG hydrogels with PEI 25K as a positive control, normalized to that obtained on TCPS ($n = 3$).

related to the crosslinking density of the hydrogels. An increase in the crosslinking density usually results in a decrease in the swelling ratio.[51] The results suggested that, in our experimental range, the increases in the H_2O_2 and HRP concentrations led to the increase in the crosslinking density, which is coincident with the SEM observation (Fig. 5).

In vitro cytocompatibility

L929 mouse fibroblasts were incubated inside the PLG-*g*-TA/PEG hydrogels formed with different concentrations of H_2O_2 and 2 units per mL of HRP. The cell viability was then determined using a live–dead cell staining kit. Cells were stained with calcein-AM/PI and observed using a fluorescent microscope. As shown in Fig. 7a, most of the cells inside the hydrogels were stained green, indicating a high viability of the cells. The cell proliferation in the PLG-*g*-TA/PEG hydrogels was analyzed by a cell counting kit-8 (CCK-8) method. The L929 cells in the hydrogel with a lower H_2O_2 concentration exhibited a higher proliferation rate (Fig. 7b), which may due to a higher porosity. The cytotoxicity of the hydrogels and any leachable materials was also evaluated by using MTT assay. The cell viability was over 90% after incubation with the eluent of the hydrogels, suggesting good cytocompatibility of the hydrogels (Fig. 7c). It is worth mentioning that the low dose of H_2O_2 used in the PLG-*g*-TA/PEG hydrogels and the mild enzyme-mediated gelation process should contribute to the excellent cytocompatibility of the hydrogels.[52,53]

Fig. 8 *In vivo* hydrogels status at different periods. PLG-*g*-TA/PEG solutions in PBS (10% (w/v)) containing H_2O_2 (1.6 mM) and HRP (2 units per mL) were subcutaneously injected into rats. Photos were taken at 15 min (0 day), 4, 10, and 14 weeks.

In vivo degradation and biocompatibility

In order to investigate the *in vivo* degradation and biocompatibility of the PLG-*g*-TA/PEG hydrogels, 500 μL of PLG-*g*-TA/PEG solution in PBS containing H_2O_2 (1.6 mM) and HRP (2 units per mL) was injected into the subcutaneous layer of rats. It was found that the hydrogels were rapidly formed *in situ* after subcutaneous injection of the PLG-*g*-TA/PEG solutions (Fig. 8). The hydrogels persisted for up to 10 weeks *in vivo*, and completely degraded 14 weeks post-injection. The PLG-*g*-TA/PEG hydrogels in the subcutaneous layer of the rats were mainly degraded due to the effects of mammalian proteolytic enzymes.[54,55]

Additionally, to investigate the biocompatibility of the hydrogels *in vivo*, the inflammatory response to the injected hydrogels was studied by hematoxylin and eosin (H&E) staining of the surrounding tissues at different time intervals. An elevated number of inflammatory cells were observed at first four weeks after injection (Fig. 9), indicating mild inflammatory reaction in the initial stage.[56,57] Notably, inflammatory cells markedly reduced and the inflammatory reaction eliminated gradually along with the degradation of the hydrogels.

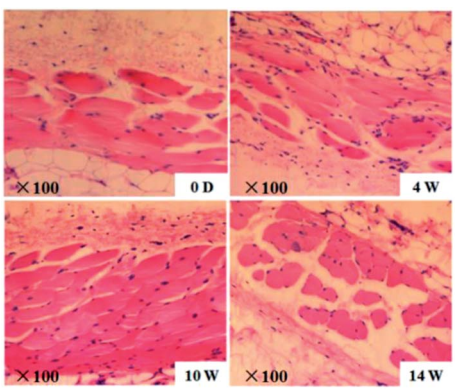

Fig. 9 Histological images of tissues around the injection sites at the back of rats (H&E staining).

Moreover, during our experiment, neither obvious tissue necrosis, edema, hyperemia and hemorrhaging nor muscle damage was observed. Therefore, the results suggested that the PLG-*g*-TA/PEG hydrogels exhibited acceptable biocompatibility *in vivo*, indicating that the hydrogels have potential in some biomedical applications, such as tissue engineering scaffolds and carriers for long-term sustained delivery of drugs and bioactive molecules.

Conclusions

A kind of enzyme-mediated injectable hydrogel based on poly(L-glutamic acid) grafted with tyramine and poly(ethylene glycol) (PLG-*g*-TA/PEG) was developed. The hydrogels were rapidly formed under physiological conditions in the presence of HRP and H_2O_2. The gelation time could be adjusted by varying the concentrations of HRP and H_2O_2. The physicochemical properties of the hydrogels, including mechanical strength, swelling ratio and porous structure, were dependent on the concentrations of HRP and H_2O_2. The live–dead staining and cell counting kit-8 revealed that the PLG-*g*-TA/PEG hydrogels exhibited good cytocompatibility *in vitro*. The *in situ* formed hydrogels in the subcutaneous layer of rats persisted for up to 10 weeks and displayed acceptable biocompatibility *in vivo*. Therefore, the PLG-*g*-TA/PEG hydrogels could be promising candidates for biomedical applications, such as tissue engineering scaffolds and carriers for long-term sustained delivery of bioactive molecules.

Acknowledgements

The authors are grateful for the financial support from the National Natural Science Foundation of China (projects 51003103, 21174142, 51073154, 51233004 and 51321062) and the Ministry of Science and Technology of China (International cooperation and communication program 2011DFR51090).

Notes and references

1 D. Y. Ko, U. P. Shinde, B. Yeon and B. Jeong, *Prog. Polym. Sci.*, 2014, **38**, 672–701.
2 N. Annabi, A. Tamayol, J. A. Uquillas, M. Akbari, L. E. Bertassoni, C. Cha, G. Camci-Unal, M. R. Dokmeci, N. A. Peppas and A. Khademhosseini, *Adv. Mater.*, 2014, **26**, 85–124.
3 J. Thiele, Y. Ma, S. M. C. Bruekers, S. Ma and W. T. S. Huck, *Adv. Mater.*, 2014, **26**, 125–148.
4 C. He, S. W. Kim and D. S. Lee, *J. Controlled Release*, 2008, **127**, 189–207.
5 L. Yu and J. Ding, *Chem. Soc. Rev.*, 2008, **37**, 1473–1481.
6 J. N. Hunt, K. E. Feldman, N. A. Lynd, J. Deek, L. M. Campos, J. M. Spruell, B. M. Hernandez, E. J. Kramer and C. J. Hawker, *Adv. Mater.*, 2011, **23**, 2327–2331.
7 M. Lemmers, J. Sprakel, I. K. Voets, J. van der Gucht and M. A. Cohen Stuart, *Angew. Chem.*, 2010, **122**, 720–723.
8 G. Song, L. Zhang, C. He, D.-C. Fang, P. G. Whitten and H. Wang, *Macromolecules*, 2013, **46**, 7423–7435.
9 Z. Zhang, J. Ni, L. Chen, L. Yu, J. Xu and J. Ding, *Biomaterials*, 2011, **32**, 4725–4736.
10 A. Gutowska, B. Jeong and M. Jasionowski, *Anat. Rec.*, 2001, **263**, 342–349.
11 H. Cui, J. Shao, Y. Wang, P. Zhang, X. Chen and Y. Wei, *Biomacromolecules*, 2013, **14**, 1904–1912.
12 K. T. Nguyen and J. L. West, *Biomaterials*, 2002, **23**, 4307–4314.
13 H. Park, X. Guo, J. S. Temenoff, Y. Tabata, A. I. Caplan, F. K. Kasper and A. G. Mikos, *Biomacromolecules*, 2009, **10**, 541–546.
14 A. S. Sawhney, C. P. Pathak and J. A. Hubbell, *Macromolecules*, 1993, **26**, 581–587.
15 C. Hiemstra, L. J. van der Aa, Z. Zhong, P. J. Dijkstra and J. Feijen, *Macromolecules*, 2007, **40**, 1165–1173.
16 C. Hiemstra, L. J. van der Aa, Z. Zhong, P. J. Dijkstra and J. Feijen, *Biomacromolecules*, 2007, **8**, 1548–1556.
17 G. N. Grover, J. Lam, T. H. Nguyen, T. Segura and H. D. Maynard, *Biomacromolecules*, 2012, **13**, 3013–3017.
18 L. S. M. Teixeira, J. Feijen, C. A. van Blitterswijk, P. J. Dijkstra and M. Karperien, *Biomaterials*, 2012, **33**, 1281–1290.
19 M. Kurisawa, J. E. Chung, Y. Y. Yang, S. J. Gao and H. Uyama, *Chem. Commun.*, 2005, 4312–4314.
20 F. Lee, J. E. Chung and M. Kurisawa, *Soft Matter*, 2008, **4**, 880–887.
21 F. Lee, J. E. Chung and M. Kurisawa, *J. Controlled Release*, 2009, **134**, 186–193.
22 S. Sakai and K. Kawakami, *Acta Biomater.*, 2007, **3**, 495–501.
23 S. Sakai and K. Kawakami, *J. Biomed. Mater. Res., Part A*, 2008, **85A**, 345–351.
24 R. Jin, C. Hiemstra, Z. Y. Zhong and J. Feijen, *Biomaterials*, 2007, **28**, 2791–2800.
25 R. Jin, L. S. M. Teixeira, P. J. Dijkstra, C. A. van Blitterswijk, M. Karperien and J. Feijen, *Biomaterials*, 2010, **31**, 3103–3113.
26 R. Jin, L. S. M. Teixeira, P. J. Dijkstra, C. A. van Blitterswijk, M. Karperien and J. Feijen, *J. Controlled Release*, 2011, **152**, 186–195.
27 R. Jin, L. S. M. Teixeira, P. J. Dijkstra, Z. Y. Zhong, C. A. van Blitterswijk, M. Karperien and J. Feijen, *Tissue Eng., Part A*, 2010, **16**, 2429–2440.
28 K. M. Park, K. S. Ko, Y. K. Joung, H. Shin and K. D. Park, *J. Mater. Chem.*, 2011, **21**, 13180–13187.
29 S. Sakai, K. Hirose, K. Taguchi, Y. Ogushi and K. Kawakami, *Biomaterials*, 2009, **30**, 3371–3377.
30 L. S. Wang, J. E. Chung, P. P. Y. Chan and M. Kurisawa, *Biomaterials*, 2010, **31**, 1148–1157.
31 L. S. Wang, C. Du, J. E. Chung and M. Kurisawa, *Acta Biomater.*, 2012, **8**, 1826–1837.
32 R. Jin, L. S. M. Teixeira, P. J. Dijkstra, M. Karperien, C. A. van Blitterswijk, Z. Y. Zhong and J. Feijen, *Biomaterials*, 2009, **30**, 2544–2551.
33 E. Lih, J. S. Lee, K. M. Park and K. D. Park, *Acta Biomater.*, 2012, **8**, 3261–3269.
34 S. Sakai, Y. Yamada, T. Zenke and K. Kawakami, *J. Mater. Chem.*, 2009, **19**, 230–235.

35 N. Q. Tran, Y. K. Joung, E. Lih and K. D. Park, *Biomacromolecules*, 2011, **12**, 2872–2880.
36 N. Q. Tran, Y. K. Joung, E. Lih, K. M. Park and K. D. Park, *Biomacromolecules*, 2010, **11**, 617–625.
37 I. Jun, K. M. Park, D. Y. Lee, K. D. Park and H. Shin, *Macromol. Res.*, 2011, **19**, 911–920.
38 K. M. Park, Y. M. Shin, Y. K. Joung, H. Shin and K. D. Park, *Biomacromolecules*, 2010, **11**, 706–712.
39 Y. K. Joung, S. S. You, K. M. Park, D. H. Go and K. D. Park, *Colloids Surf., B*, 2012, **99**, 102–107.
40 K. M. Park, Y. Lee, J. Y. Son, D. H. Oh, J. S. Lee and K. D. Park, *Biomacromolecules*, 2012, **13**, 604–611.
41 T. J. Deming, *Prog. Polym. Sci.*, 2007, **32**, 858–875.
42 C. He, X. Zhuang, Z. Tang, H. Tian and X. Chen, *Adv. Healthcare Mater.*, 2012, **1**, 48–78.
43 Y. Cheng, C. He, C. Xiao, J. Ding, X. Zhuang, Y. Huang and X. Chen, *Biomacromolecules*, 2012, **13**, 2053–2059.
44 C. Deng, J. Wu, R. Cheng, F. Meng, H.-A. Klok and Z. Zhong, *Prog. Polym. Sci.*, 2014, **39**, 330–364.
45 C. He, C. Zhao, X. Chen, Z. Guo, X. Zhuang and X. Jing, *Macromol. Rapid Commun.*, 2008, **29**, 490–497.
46 P. Y. Myer, *Macromolecules*, 1969, **2**, 624–628.
47 Y. Ogushi, S. Sakai and K. Kawakami, *J. Biosci. Bioeng.*, 2007, **104**, 30–33.
48 S. Sakai, Y. Ogushi and K. Kawakami, *Acta Biomater.*, 2009, **5**, 554–559.
49 B. Halliwell, M. V. Clement and L. H. Long, *FEBS Lett.*, 2000, **486**, 10–13.
50 A. Leal-Egaña, A. Díaz-Cuenca and A. R. Boccaccini, *Adv. Mater.*, 2013, **25**, 4049–4057.
51 X. Gao, Y. Cao, X. Song, Z. Zhang, X. Zhuang, C. He and X. Chen, *Macromol. Biosci.*, 2014, **14**, 567–575.
52 R. Jin, C. Lin and A. Cao, *Polym. Chem.*, 2014, **5**, 391–398.
53 R. Jin, B. Lou and C. Lin, *Polym. Int.*, 2013, **62**, 353–361.
54 C. Li, *Adv. Drug Delivery Rev.*, 2002, **54**, 695–713.
55 L. S. Nair and C. T. Laurencin, *Prog. Polym. Sci.*, 2007, **32**, 762–798.
56 Y. Cheng, C. He, C. Xiao, J. Ding, H. Cui, X. Zhuang and X. Chen, *Biomacromolecules*, 2013, **14**, 468–475.
57 E. Y. Kang, H. J. Moon, M. K. Joo and B. Jeong, *Biomacromolecules*, 2012, **13**, 1750–1757.